115

Behavior of High Burnup Fuel Rod Cladding during Long-term Dry Storage in CASTOR® Casks

A. Schaberg [a], H. Spilker [a], W. Goll [b]

[a] *Gesellschaft für Nuklear-Behälter mbH, P.O.Box 101253, 45012 Essen, Germany*
[b] *Siemens AG, Power Generation Group (KWU), P.O. Box 3220, 91050 Erlangen, Germany*

This study was performed by order and in co-operation with the German utilities.

ABSTRACT

Short-time creep and rupture tests were performed to assess the strain potential of cladding of high burnt fuel rods under conditions of dry storage. The tests comprised optimized Zry-4 cladding samples from fuel rods irradiated to burnups of up to 64 MWd/kgU and were carried out at temperatures of 573 and 643 K at cladding stresses of about 400 and 600 MPa. The stresses, much higher than those occurring in a fuel rod, were chosen to reach circumferential elongations of about 2 % within an envisaged testing time of 3-4 days. The creep tests were followed by a low temperature test at 423 K and 100 MPa to assess the long-term behavior of the cladding ductility especially with regard to the effect of a higher hydrogen content in the cladding due to the high burnup.

The creep tests showed considerable uniform plastic elongations at these high burnups. It was demonstrated that around 600 K a uniform plastic strain of at least 2 % is reached without cladding failure.

The low temperature tests at 423 K for up to 5 days revealed no cladding failure under these conditions of reduced cladding ductility. It can be concluded that the increased hydrogen content has no adverse effect on the cladding performance.

1. INTRODUCTION

The general tendency to higher discharge burnups of LWR fuel assemblies has also to be considered at the back end of the fuel cycle. In Germany, dry storage is a settled technology for interim storage. Two central interim storage sites are licensed and further installations near the reactor sites have been applied for by the electric power utilities. For long-term dry storage of spent fuel assemblies (FA) in casks a proof is to be furnished, that a systematic rod cladding failure during storage will not occur.

Over the last years, however, the enrichment and consequently the discharge burnup of the FAs in the light water reactor has been increased continuously among other things by introducing high corrosion resistant materials and advanced licensing methods /1/. Since dry storage is gaining more and more importance for interim storage, it has been of interest to assess the creep-rupture behavior of the zirconium cladding used for high burnup fuel rods. High burnup means, increased neutron fluence and hydride content from the cladding corrosion due to long insertion times at high thermal power.

Early investigations on the mechanical properties of stress relieved and recrystallized cladding tubes have shown that burst strength and burst elongation reach a saturation level and that differences diminish at fast fluences above $4\text{-}6\cdot10^{21}cm^{-2}$ /2/. Therefore, a further increase of the fluence is not expected to have a detrimental influence on the cladding mechanical behavior.

Hydrogen is produced during the corrosion reaction and, with increasing oxide layer thickness, an increased amount of hydrogen is found in the cladding. The properties of hydrides in zirconium and its alloys is gathered in /3/. If a solubility limit of e.g. about 150 ppm at operating temperature is exceeded, the hydrogen will precipitate as ZrH-platelets. The δ-phase is assumed to be the dominant phase especially under slow cooling reactor conditions. The orientation of the precipitates in the cladding will depend on texture and stress during precipitation.

The amount of hydrogen in the cladding and the orientation of the precipitates relative to the stress applied can reduce the tensile strength and the ductility compared with hydrogen-free material. At elevated temperatures the effect of the hydrogen on the ductility is less pronounced than it is at room temperature /4-7/. In case of irradiated materials the irradiation effect dominates the ductility up to hydrogen contents of at least 1000 ppm /8/.

With regard to interim dry storage, a certain range of operational parameter has to be considered /9/. Due to the irradiation and cask storage conditions, the maximum cladding stresses are 100-120 N/mm^2 at the beginning of storage and the temperatures range from 400°C down to 200 °C after tens of years. This means that the cladding is mainly operated in a regime of low hydride reorientation (<100 N/mm^2) and above the ductile-brittle transition (> 200 °C) /3/.

The short-time creep tests were supplemented by creep tests on unirradiated cladding materials. The perspective of these tests was to describe conservatively the post-pile creep of

irradiated cladding by the creep of unirradiated cladding in order to prevent fuel rod degradation by limiting the cladding hoop strain /10/.

The short-time creep tests on irradiated cladding were geared to demonstrate the strain capability of high burnup cladding and the cladding integrity under realistic cladding hydrogen concentrations. Therefore, the test was divided into two different tests. The first test consisted of a creep test. It was performed with the objective of reaching a plastic hoop strain of about 2 % within several days, this means much faster than under conditions of dry storage but at comparable storage temperatures of 573 and 643 K. The creep test was followed by a ductility test in which the cladding was slowly cooled down to 423 K and held at a stress of 100 MPa for up to 5 days.

The test device was developed and installed at the Institute for Transuranium Elements (ITU) at Karlsruhe, Germany.

2. MATERIALS

The cladding material used in the tests was prepared from two standard fuel rods with an outer diameter of 10.75 mm and a wall thickness of 0.73 mm. The cladding consisted of corrosion optimized Zircaloy-4 with 1.29 w/o Sn, 0.22 w/o Fe, and 0.12 w/o Cr. The annealing parameter was about $2.2 \cdot 10^{-17}$ h. In the as-fabricated state the cladding had a tensile strength of 776 N/mm^2 at room temperature and of 423 N/mm^2 at 673 K. The rods A and B were irradiated in a commercial PWR for four and five irradiation cycles up to rod average burnups of 54 and 64 MWd/kgU equivalent to neutron fluences of $9.5 \cdot 10^{21}$ and $12.1 \cdot 10^{21}$ cm^{-2} (E_n>1 MeV), respectively.

The irradiation behavior of the rods was deduced from non-destructive examinations performed on rod B and on comparable rods.

The diameter change of rods from the same batch is shown in Fig. 1 as a function of the burnup. It can be seen that the cladding of rod A experienced a maximum diameter decrease of 0.8 - 0.9 %, whereas cladding of rod B was additionally strained back by about 0.2 % Fig. 2 shows the axial oxide layer profiles of the rods. The oxide layer of rod B was measured nondestructively by the eddy current technique and circumferentially averaged over an axial length of 40 mm. The axial oxide layer profile of rod A was estimated from a comparable oxide layer profile that was adjusted by means of oxide layer thicknesses obtained metallographically at three axial rod positions.

It can be seen that rod A had an oxide layer thickness of up to 47 µm and rod B a layer thickness of up to 100 µm.

3. EXPERIMENTAL SETUP

3.1 Equipment design

The system is based on the internal pressurization of a cylindrical sample and is able to perform creep- as well as burst-tests. Oil (stiff system) was preferred to gas (soft system) pressurization because its intrinsic lower stored energy. In Fig. 3 a schematic diagram of the apparatus is shown. The system, allowing to reach pressures up to about 200 MPa, is situated outside the hot cell and is connected to the sample through an pipe-line system.

The dual piston pump allows a constant rate of pressure increase in the sample. The pumping rate can be varied in order to avoid that a pressure surge will be produced during a pump stroke or the overloading of the system due to inertia. During the a test, a computer controls the pump; the pumping rate is set to the minimum and the software assures a constant pressure to within ±1 bar during the whole test.

A data taking system allows the simultaneous recording of the specimen pressure, as measured by a pressure transducer located near to the sample, the oil volume input to the specimen, obtained from the piston travel via a potentiometer transducer, and the temperature of the sample. At pre-set intervals (usually every 10 minutes), the instant values of the pressure, temperature and piston displacement can be recorded during the whole test.

As pressurization fluid a silicon oil (Dow Corning 200) was used, having an expansion coefficient of 1.34×10^{-3} ml/ml °C and a compression coefficient ($\Delta V/V_o$) of about 0.2 at room temperature. In the closed system used, the stability of the oil was not affected by the temperature and no cracking and/or oxidation phenomena were observed.

An electrical furnace, having three heating zones and provided with an internal double wall lining containing Cs, allows the homogeneous heating of the sample to the test temperatures. During the test, a gradient along the whole sample length less than ± 0.2 °C could be achieved. The temperature gradient is checked by means of two thermocouples attached to the upper and lower grips and a third positioned near to the center of the sample. The temperature control system allows an accuracy within ± 2 °C of the test temperature.

The equipment was designed for samples, having variable diameter, up to 150 mm in length which, taking into consideration the grip length, insures an unsupported length of about 10 times the average outside diameter, as recommended in the ASTM – Norm B 353.

3.2 Ancillary equipment

Three devices were developed in order to: a) remove the fuel, b) tighten the specimen grips and c) measure the sample diameter, previous and after the testing.

3.2.1 Fuel removal and sample preparation

Based on a commercial drilling machine, able to hammer while drilling, a device was developed to remove the fuel from the segments of irradiated fuel rods, Fig. 4. The device uses a hard metal drilling tool, fixed during the operation while the samples rotates. The system allows a smooth vertical displacement through counterweights which maintains the sample in quasi-equilibrium during the whole operation.

The diameter of the drilling tool was around 1 mm smaller than the nominal internal diameter of the sample. Considering that the fuel-cladding interaction at the burnups of interest (more than 50 GWd/tU) can be large, an additional technique was developed to partially remove the interaction layer in the grip zones. To this goal, a lathe – modified to be used under remote controlled conditions – provided with special grinding tools was used (see below).

3.2.2 Tightening device

Mechanically attached end-fittings were used to seal the specimen. In order to screw the fittings, a special device was developed on the basis of a commercial pneumatic wrench, able to perform a smooth tightening of the fittings, thereby avoiding impacting of pulsing tightening cycles which could lead to the damage of the samples. The maximum achievable torque is around 500 N/m.

The torque can be controlled to within ± 5% of the target by regulating the gas pressure. The samples were strengthened by inside mandrels in order to support, at least partially, the external forces applied during the tightening of the metallic seals. The mandrels are provided with a groove to facilitate the displacement of the fluid within the specimen.

3.2.3 Sample measurement

A displacement transducer (LVDT) has been mounted on a floating head to measure the relative movement of two knives, which perform the measurements using as reference calibrated standards. The device is able to detect variations of ± 0.1 μm in the diameter. The apparatus also performs the measurement of the axial displacement (± 0.01 mm), allowing the correlation of the diameter measurement to the axial position on the sample.

3.3 Specimen preparation

Special care was exercised during the drilling operation to avoid damage of the sample wall or to cause the deformation of the sample. Drilling periods were alternated with inactive intervals, to avoid the sample heat-up during the drilling procedure.

A lathe was used to remove the remained fuel and, partially, the interaction layer. The internal diameter of the sample was then measured by calibrated gauges and the value used to machine the internal mandrel with a typical tolerance of – 20 μm. Finally, the fuel segments were externally treated with a fine emery paper and visually inspected to ascertain that neither undercuts nor scratches were present on the surface. Finally, before the test the samples were

measured, usually in five axial and in four azimuthal positions, to determine possible eccentricities.

3.4 Test schedule

A precise schedule had to be established for the tests. This includes: a) the pre-loading of the sample during the heating phase, in order to avoid the seeding of the oil in the sample; b) an accurate elimination of the occluded air, to keep the stored energy low and to have a reliable measurement of the strain through the amount of oil pumped into the sample; c) the pressurization of the creep samples was performed only after the test temperature was achieved and remained stable; and, d) a pre-heating phase at low pressure, lasting two hours, was used as the standard procedure.

4. TESTS

Fig. 5 shows the schematic sequence of the tests for a maximum temperature of 643 K. The test with a maximum temperature of 573 K was carried out in the same way. Both tests were designed to reach a plastic hoop strain of about 2 % within 3 to 4 days. The appropriate pressure was chosen accordingly and the sample pressurized with a rate less than 35 MPa/min. The strain rate was determined from the change of the oil inventory and the pressure slightly corrected if necessary.
In case of intact samples, the creep phase was followed by a ductility test at 423 K and reduced pressure (100 MPa). The ductility test was planned to last up to about 5 days.

5. RESULTS

The results of the creep tests on the rods A and B are presented in Figs. 6 and 7. The cladding stress needed to achieve the required creep rate was in the range of 400 to 430 MPa at 643 K and of about 600 MPa at 573 K. At 643 K the samples reached uniform plastic elongations between 0.3 and 7.4 %. The low value of 0.3 % resulted from an early defect in the clamping region. At 573 K the range of uniform plastic elongation was 1.0 to 3.5 %. In this case of low temperature, it was difficult to maintain the tightness of the clamping for a sufficient long time.

The results are plotted in Fig. 8. It can be seen that no cladding failure occurred below 2 % uniform plastic strain. Above 2 % elongation, rupture was observed on six out of fifteen samples. Before failure, the elongation vs. time curve derived from the oil inventory, always showed that the samples were in ternary creep stage, Fig. 9. This is an indication for high local ductility of the cladding. A systematic influence of oxide layer and hydrogen content on the creep behavior was not detected.

All intact samples were submitted to a ductility test at 423 K to test the influence of the hydrogen at low temperatures and the effects of cladding stresses comparable to those found in high burnup rods due to their internal pressure. All samples tested remained intact.

The behavior of the hydrogen in the cladding was investigated by metallographic examinations performed after testing. Fig. 10 shows the hydride distribution of the intact sample A_3b tested at 573 K. The tangentially orientated platelets reflect the typical distribution immediately after discharge from the reactor.

During testing at 573 K part of the platelets was dissolved and precipitated under stress (100 MPa) during the cool down phase of about 3 h for the ductility test. This led to the precipitation of radially orientated platelets, however, without cladding failure.

6. CONCLUSIONS

The short-time creep and rupture tests have shown that corrosion optimized Zry-4-cladding of high burnt rods can reach 2% plastic strain under the very high stresses of 400 to 600 MPa. Such a high strain without cladding degradation is a comfortable basis, especially with regard to a licensed level of 1% /11/. Thus, other cladding types with base materials of lower creep are also covered, if a creep model based on an enveloping, fast creeping material is used.

The cladding material with a realistic hydrogen distribution was tested under simulated low-ductile conditions, i.e. cladding stress of 100 MPa and a temperature of 423 K. For dry storage conditions this combination of stress and temperature is very unlikely to occur and, hence, can be regarded as conservative. So, it can be expected that under realistic long-term cooling conditions no hydrogen-induced effects should degrade the cladding integrity.

Acknowledgement:

This work was funded by the German utilities. We would like to thank the utility group 'Fuel Assembly Cladding Behavior' for their cooperation and useful discussions.

7. LITERATURE

/1/ H. Gross, P. Urban, 'Technical and Licensing Challenges and their Solutions for High Burnup', TOPFUEL '99, Avignon, France, 13-15 September 1999, p. 262

/2/ F. Garzarolli, R. Manzel, H. Schönfeld, E. Steinberg, 'Influence of Final Annealing on Mechanical Properties of Zircaloy Before and After Irradiation', 6th SMIRT Conf. Paris, 1981, C2/1

3/ D.O. Northwood, U. Kosasih, 'Hydrides and Delayed Hydrogen Cracking in Zirconium and its Alloys', International Metals Reviews, 1983, Vol.28, No.2, p.9

/4/ D.S. Wood, J. Winton, B. Watkins, 'Effect of Irradiation on the Impact Properties of Hydrided Zircaloy-2 and Zirconium-Niobium Alloy,' Electrochemical Technology 4(1966)250-258

/5/ G.D. Fearnehough, A. Cowan, 'The Effect of Hydrogen and Strain Rate on the 'Ductile-Brittle' Behaviour of Zircaloy', Journal of Nuclear Materials 22 (1967)137-147

/6/ J. Bai, C. Prioul, J. Pelchat, F. Barcelo, 'Effect of Hydrides on the Ductile-Brittle Transition in Stress-Relieved, Recrystallized and Beta-Treated Zircaloy-4', ANS/ENS Topical Meeting on Light Water Reactor Fuel Performance – April 1991, p.233-241

/7/ S. -Q. Shi, M.P Puls, 'Fracture Strength of Hydride Precipitates in Zr-2.5Nb Alloys', Journal of Nuclear Materials 275(1999)312-317

/8/ W. Jahreiß, R. Manzel, E. Ortlieb
'Einfluß des Wasserstoffgehaltes und der Bestrahlung auf das mechanische Verhalten von Brennelementstrukturteilen aus Zircaloy',
Jahrestagung Kerntechnik '93, 25. - 27. Mai 1993, Seite 303 ff.

/9/ M. Peehs, F. Garzarolli and W. Goll,
'Assessment of Dry Storage Performance of Spent LWR Fuel Assemblies with Increasing Burn-up', International Symposium on Storage of Spent Fuel From Power Reactors, Vienna, 9 - 13 November 1998

/10/ H. Spilker, M. Peehs, H.-P. Dyck, G. Kaspar, K. Nissen, 'Spent LWR Fuel Dry Storage in Large Transport and Storage Casks After Extended Burnup', Journal of Nuclear Materials 250 (1997) 63-74

/11/ W. Sowa, D. Hoffmann, B. Lorenz, 'Die Aufbewahrungsgenehmigungen für die Transportbehälterlager Ahaus und Gorleben', Jahrestagung Kerntechnik 1998, S. 265

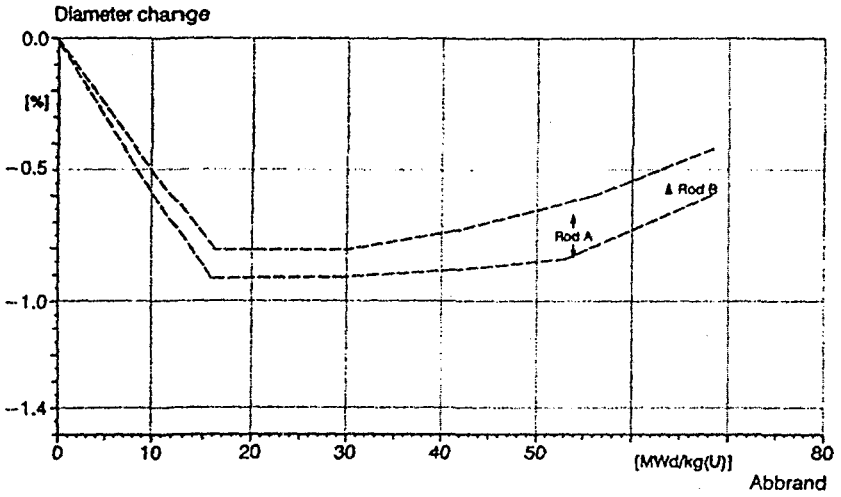

Fig. 1 Diameter Behavior of the Cladding During Reactor Operation

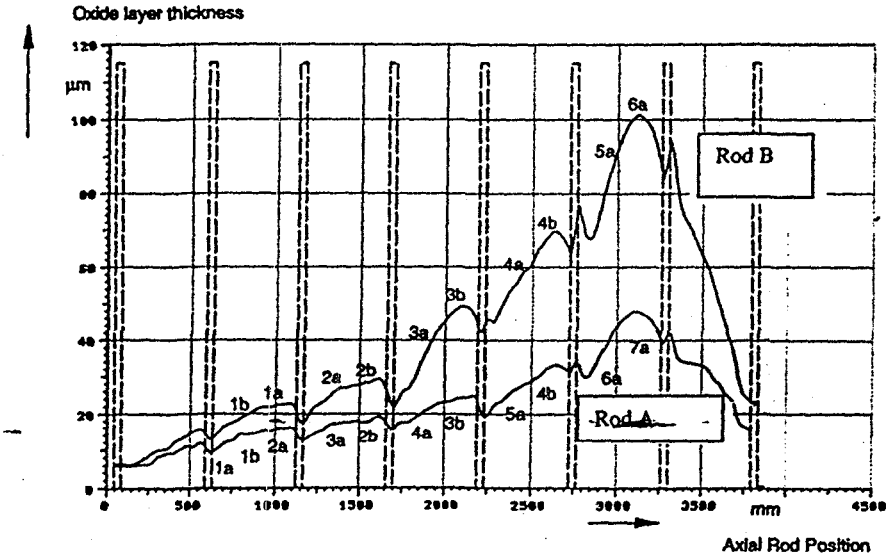

Fig. 2 Axial Oxide Layer Ticknesses of Rod A and B and Sample Positions

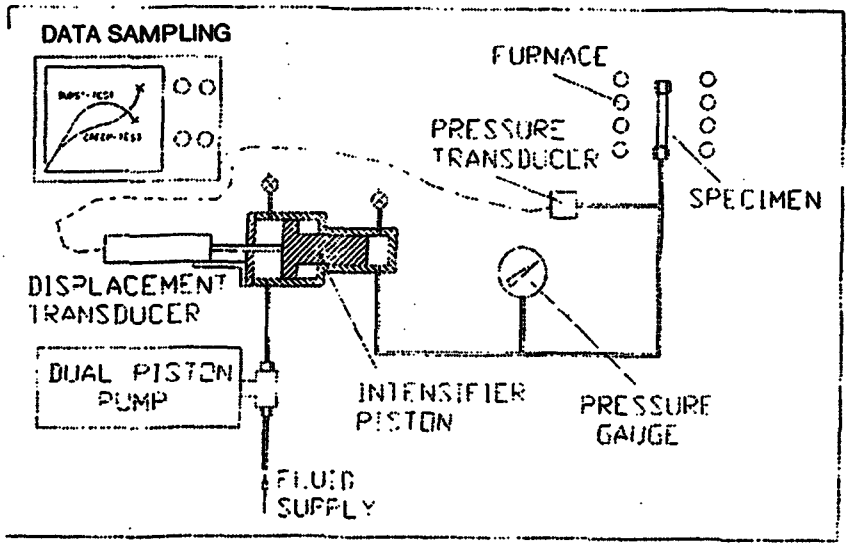

Fig. 3 Schematic Measurement Device

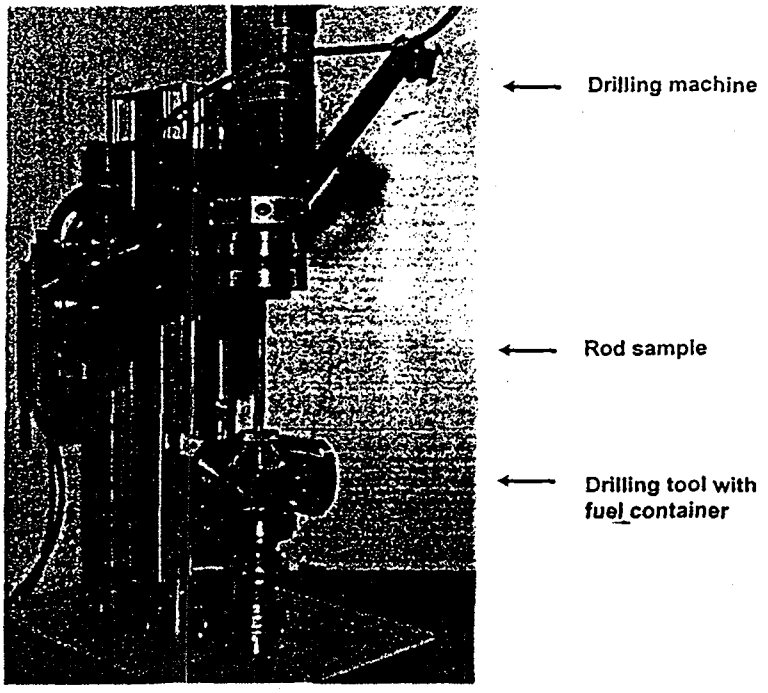

Fig. 4 Fuel Removal Device

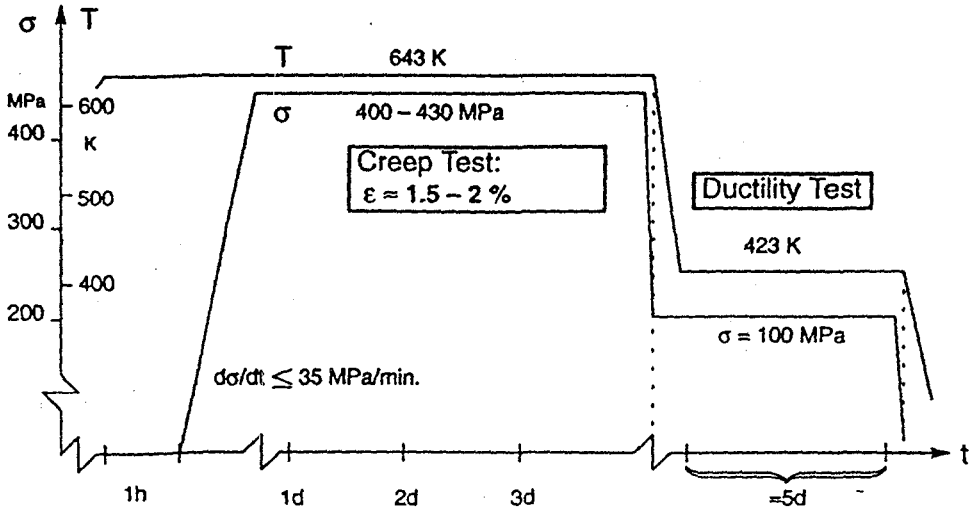

Fig. 5 Testing Sequence

Rod-Designation	Test Conditions Stress MPa	Time h	Uniform Plastic Elongation %	Ductility Test 100 Mpa, 423 K Time h	Comment
	Temp. 643 K				
A_1a	320	72	4.5	90	Sample intact
A_2a	430	30	7.4	100	Sample intact
A_3a	430	2	0.3		Clamping failed
A_4a	430	54	4.2	62	Sample intact
A_5a	400	129	≈ 6*		Sample failed
A_6a	410	74	2.3	89	Sample intact
A_7a	410	67	≈ 4.5*		Sample failed
	Temp. 573 K				
A_1b	630	65	1.2		Clamping unstable
A_2b	620	44	1.0	109	Sample intact
A_3b	620	189	2.4	26	Sample intact
A_4b	620	69	3.5	92	Sample intact

* averaged over intact region

Fig. 6 Results of the Creep Tests on Rod A Samples

Rod-Designation	Test Conditions		Uniform Plastic Elongation	Ductility Test 100 Mpa, 423 K Time	Comment
	Stress MPa	Time h	%	h	
	Temp. 643 K				
B_1a	400	100	2.5	90	Sample intact
B_2a	400	124	3.1	63	Sample intact
B_3a	420	111	4.1	119	Sample intact
B_4a	410	137	4-6*		Sample failed
B_5a	400	88	≈ 5*		Sample failed
B_6a	410	55	3.0		Sample failed
	Temp. 573 K				
B_1b	620	143	1.9	120	Sample intact
B_2b	620	143	1.1	97	Sample intact
B_3b	620	119	1.4		Defect near clamping
B_4b	630	13	≥ 2.5		Repaired sample failed

* averaged over intact region

Fig. 7 Results of the Creep Tests on Rod B Samples

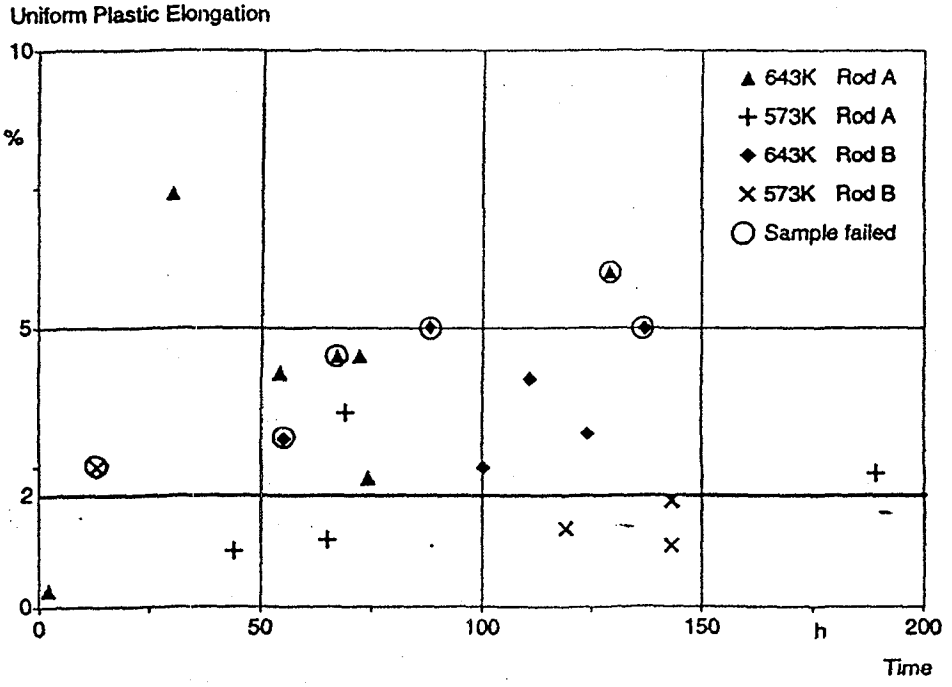

Fig. 8 Results of Uniform Plastic Strain

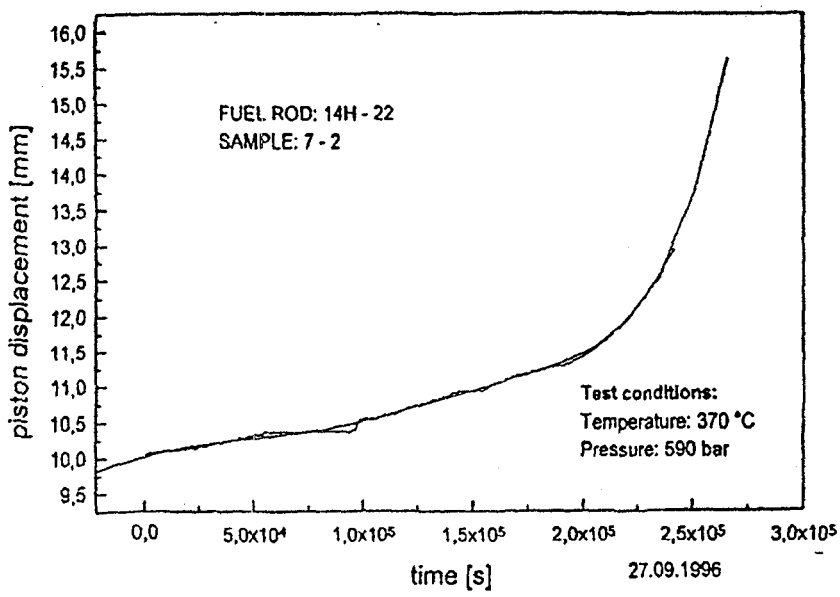

Fig. 9 Piston Displacement Until Sample Rupture

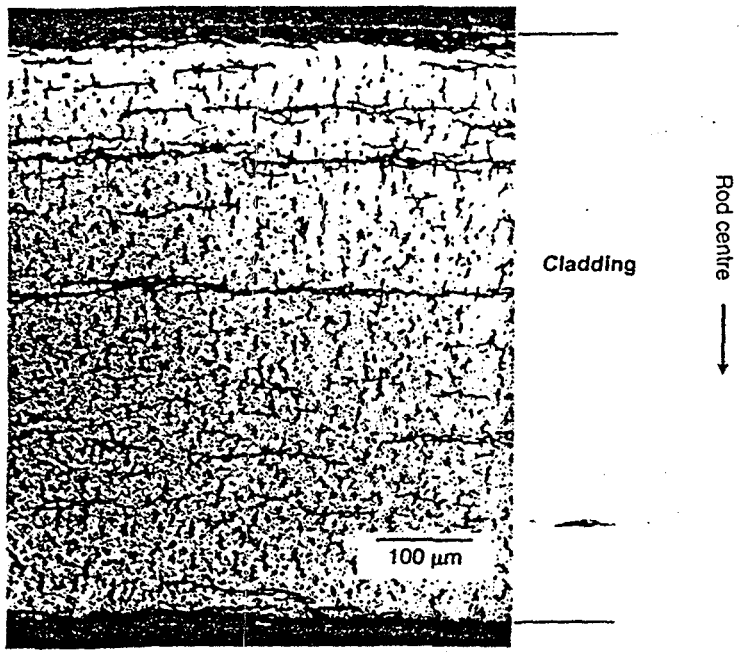

Fig. 10 Metallographic Examination of Sample A_3b after 573K-Creep and 423K-Ductility Testing